

Reduction in piston-cylinder experiments: The detection of carbon infiltration into platinum capsules

RICHARD BROOKER,^{1,*} JOHN R. HOLLOWAY,¹ AND RICK HERVIG²

¹Department of Geology, Arizona State University, Tempe, Arizona 85287, U.S.A.

²Center for Solid State Science, Arizona State University, Tempe, Arizona 85287, U.S.A.

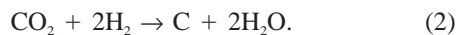
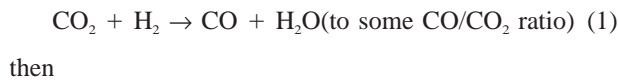
ABSTRACT

Problems associated with intermittent and variable degrees of sample blackening are often reported for studies involving the preparation of CO₂-bearing silicate glasses in piston-cylinder apparatus. This phenomenon is generally attributed to H infiltration, which leads to the reduction of CO₂ and the precipitation of graphite with the concomitant formation of water. In this study we demonstrate that carbon diffusion into platinum capsules may be a common cause of blackened glasses and this process may be detected using fourier transform infrared spectroscopy (FTIR) to identify the presence of CO without elevated H₂O contents. The simulated infiltration of ¹²C from a graphite furnace into a ¹³C-bearing sample is illustrated using secondary ion mass spectroscopy (SIMS) and micro-FTIR analysis.

Careful FTIR monitoring of variable sample reduction has helped to identify the precautions required to reduce C (and H) infiltration in solid media assemblies and it appears that physical barriers can be more important than the chemical buffers traditionally employed.

INTRODUCTION

Examples of blackened samples prepared in piston-cylinder apparatus can be found throughout the experimental literature and many petrologists will acknowledge that similar problems are often observed but not reported. For experiments where oxidized carbon species are included in the bulk composition, the blackening is generally attributed to the reduction of these species to produce graphite. It is commonly suggested that infiltration of H₂ causes graphite to precipitate by the following types of reaction:



In many experiments, the diffusion of H₂ into capsules is actually utilized to impose a controlled f_{O_2} (more correctly f_{H_2} ; see Luth 1989) during the experiment with the sample-bearing capsule being enclosed in a second sealed capsule containing the required buffer assemblage and H₂O (e.g., Eugster 1957). Reduction and the perceived entry of H₂ into single capsules that are not intentionally buffered has led to the concept of an “intrinsic f_{O_2} ” in which the pressure vessel and/or solid media assembly are thought to act as both the source and buffer of f_{H_2} .

Mysen and co-workers at the Geophysical Lab (Hol-

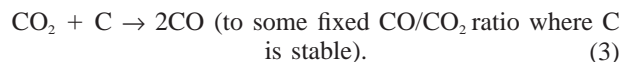
loway et al. 1976; Mysen 1976; Mysen et al. 1976) have prepared many CO₂-bearing glass samples using a talc piston-cylinder assembly without blackening of samples. This has been attributed to a high overall intrinsic f_{O_2} near the hematite-magnetite buffer for this assembly (Eggler et al. 1974). This intrinsic f_{O_2} is considerably higher than values measured in other laboratories (nickel-nickel oxide for Allen et al. 1972; below nickel-nickel oxide for Merrill and Wyllie 1974; slightly below nickel-nickel oxide for Brey and Green 1976; near wustite-magnetite for Watson et al. 1982; just below quartz-fayalite-magnetite for Watson 1987). Eggler et al. (1974) attributed the high f_{O_2} environment in their assembly to the presence of boron nitride, which may act as a sink for H₂ (see Wendlandt et al. 1982). This conclusion was apparently supported by the blackening of CO₂-bearing glasses when the boron nitride was removed from the talc assembly. However, Brey and Green (1976) suggested that Pyrex could be used successfully in place of boron nitride to reduce migration of H₂ from an outer talc sleeve to the capsule.

More recent studies of CO₂ solubility in silicate melts have favored a combination of NaCl and Pyrex in 12.7 mm assemblies. With the elimination of the talc as a source of H₂O, it might be expected that the bulk amount of H₂ available for infiltration would be reduced to an insignificant level. However, blackening still occurs in these assemblies and several workers have pursued a double capsule technique to maintain a high f_{O_2} (or low f_{H_2}) and avoid graphite formation (e.g., Boettcher 1984; Brey 1976; Brey and Green 1976; Fine and Stolper 1985; Stol-

* Current address: Department of Geology, Wills Memorial Building, University of Bristol, Bristol BS8 1RJ, U.K. E-mail: r.a.brooker@bristol.ac.uk

per et al. 1987; Matthey et al. 1990; Matthey 1991; Taylor 1990). In fact, this method actually allows some limited infiltration of H_2 giving the reaction in Equation 1, although the inner capsule reaches the f_{O_2} (f_{H_2}) imposed by the outer buffer before graphite precipitates. An example of this limited infiltration of H_2 is seen in the study of Stolper et al. (1987) who illustrate a cross section through a buffered sample showing an increase in the H_2O content and a concurrent decrease in the CO_2 concentration toward the edge of the charge. The increased H_2O concentration (0.08 wt%) and the decrease in CO_2 (0.2 wt%) are in the exact proportions to satisfy Equation 1, requiring the influx of 0.0091 wt% H_2 and the production of 0.13 wt% CO. Reports of apparent "carbon loss" (Fine and Stolper 1985) might be explained by the production of CO if this species is not identified in the quenched glass or excess fluid. Rosenbaum and Slagel (1995) have suggested that the choice of packing material used around a single capsule can have a significant effect on restricting entry of H_2 , and that soft glass or Pyrex can be at least as effective as a double capsule. However, the general concept of H_2 infiltration has remained, even though the causes and remedies are not always clear.

The experiments and observations presented in this study are complementary to an investigation of CO_2 solubility in melt compositions along the $NaAlO_2$ - SiO_2 join at 1450–1700 °C and 1.0–2.5 GPa (Brooker et al., unpublished data; see also Kohn et al. 1991). The study of Brooker et al. (unpublished data) required relatively large samples to permit a variety of analytical techniques for each experiment. It was also necessary to avoid the Fe contamination that is commonly reported for Fe oxide-buffered experiments (e.g., Brey 1976; Brey and Green 1976; Matthey et al. 1990; Taylor 1990) because this would be detrimental to nuclear magnetic resonance (NMR) analyses performed on selected samples (see Kohn et al. 1991). As a result of these constraints, experiments were attempted in large single capsules without the use of a outer Fe oxide "buffer." Over 80% of these experiments showed blackening that ranged from dusty vesicle linings and surface deposits in the higher SiO_2 compositions to darkened rims in $NaAl_2SiO_6$ (jadeite, Jd) and complete blackening of $NaAlSiO_4$ (nepheline, Ne) glasses. This blackening was attributed initially to graphite precipitation related to H_2 infiltration. However, various observations suggested that H_2 was not responsible for the reduction. The H_2O content of many blackened samples was unexpectedly low and comparable to unblackened glasses, and a number of carbon (CO_2)-free starting compositions also produced graphite-bearing samples (as confirmed by Raman spectroscopy). In addition, IR spectroscopy revealed variable levels of ^{12}C contamination in samples prepared with 99% ^{13}C -enriched starting materials. These observations indicated that C rather than H_2 might be entering the platinum capsules leading to the following reaction:



The possibility of C diffusing through Pt was originally suggested by Watson et al. (1982) and further demonstrated by Watson (1987). However, this process appears to have been ignored by many workers who consider H_2 infiltration to be the only problem and present pursue buffered double-capsule techniques.

In this study we demonstrate a method for distinguishing between H_2 and C infiltration, and suggest causes and remedies for mobility of C. The C infiltration hypothesis is tested by determining the H_2O contents of two blackened, Ne + $^{12}CO_2$ -composition glasses using FTIR spectroscopy. This allows a calculation of the mass balance, which would be related to the progress of reactions in Equations 1 and 2. In addition, glasses of initial composition Jd + $^{13}CO_2$ have been prepared in platinum capsules surrounded by secondary capsules containing ^{12}C graphite or Jd + $^{12}CO_2$. These experiments simulate two extreme cases of oxidation gradient (and C activity) across a platinum wall. The composition of the resulting samples has been determined by SIMS and FTIR spectroscopy to trace the migration of ^{12}C and ^{13}C isotopes.

EXPERIMENTAL AND ANALYTICAL PROCEDURES

Starting materials for both the Jd + $^{13}CO_2$ ($NaAlSi_2O_6$) and Ne + $^{12}CO_2$ ($NaAlSiO_4$) compositions consisted of acid-leached Brazilian quartz, reagent grade Al_2O_3 , and Na_2CO_3 or 99% ^{13}C -enriched Na_2CO_3 . The quartz and Al_2O_3 were dried at 1000 °C and stored at 120 °C, and the carbonate was dried at 500 °C immediately before loading in to the capsule. The starting compositions were weighed out and then dry-mixed in an oven at 120 °C, using a mortar and pestle. Capsules were loaded, removed from the oven, and immediately welded shut before being squashed and weighed. The platinum capsules were pre-annealed, and for the double capsule experiments, a 3 mm inner capsule containing the Jd mixture was crimp welded and then surrounded by either powdered graphite (from a crushed furnace fired at 1000 °C), or a Jd + $^{12}CO_2$ mixture. The inner capsule and the outer material were then sealed in a 5 mm, pre-annealed platinum capsule of the "ash can" design (Sneeringer and Watson 1985), which were also used for the single capsule Ne composition experiments. The capsules were loaded into the 12.7 mm solid media assembly illustrated in Figure 1. The salt parts of this assembly were annealed at 700 °C for 12 h after pressing, then stored at 120 °C along with the Pyrex sleeves. The graphite furnaces and crushable alumina parts were fired at 1000 °C+ prior to use.

The capsules in this study were surrounded by Pyrex powder. This technique has been used at Arizona State University (ASU) for some time as it allows the use of a large capsule without the need for very thin, crushable alumina sleeves that are difficult to machine. After the experiment, volatile-bearing capsules surrounded by Py-

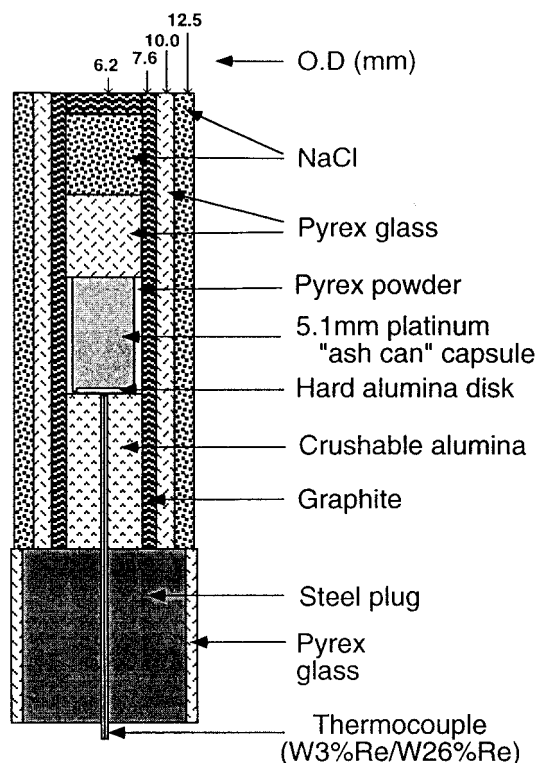


FIGURE 1. The solid media, piston cylinder assembly used in this study. Later modifications included a reduction in the diameter of the capsule (to 4.6 mm), which was then surrounded by a crushable alumina sleeve instead of crushed Pyrex. A crushable alumina disk (1 mm thick) was also placed above the capsule.

rex had a rounded, barrel-like appearance giving an audible hiss when punctured.

Mid-IR spectra were obtained at ASU on a Biorad FTIR spectrometer (digilab FTS-40). The microscope attachment on this instrument was used to analyze 50 μm square sections through doubly polished (constant thickness) plates of glass, representing horizontal sections through the experiments. Wavenumbers from 4000 to 400 cm^{-1} were scanned at 8 cm^{-1} resolution, with the signal being averaged over 256 scans.

Secondary ion mass data were obtained at ASU using a Cameca 3f ion probe, measuring spluttered, negative secondary ions generated by a primary $^{16}\text{O}^-$ beam from a duoplasmatron ion source at -12.5 kV accelerating potential. The 10 μm beam was rastered over the area to be examined to remove surface contamination before conducting spot analysis with a static beam. Peaks indicating yields for ion masses 1 (H), 12 (C), 13 (C), 16 (O), and 28 (Si) were measured at each analysis point. For a few samples, masses 18 (O) and 11 (B) were also measured. In general, the Si counts were used to normalize other masses.

RESULTS

H_2O contents

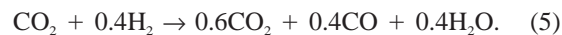
The blackened Ne samples presented in this study were considered as "failed" experiments for the purposes of the Brooker et al. (unpublished data) study, but provide useful information in the context of this paper. These Ne samples were completely blackened and visibly opaque at a thickness of 2 mm, but it was possible to see through the samples thinned to <200 μm and therefore to obtain IR spectra. The IR spectrum of an Ne sample prepared at 1.5 GPa and 1650 $^\circ\text{C}$ is illustrated in Figure 2a. The IR spectra for the 2.5 GPa samples indicate a CO_2 content in excess of 5 wt% and an H_2O content of ~ 0.1 wt%; with such a disparity it is difficult to see the H_2O peak when the carbonate doublet is on scale, and for presentation purposes these spectra have not been included in Figure 2a. It should be noted that the Ne samples prepared at 2.5 GPa and 1650 $^\circ\text{C}$ contained a very small amount of crystalline nepheline at one end of the charge, although this was easily avoided during IR analysis.

Although only a minor feature in Figure 2a, a small amount of dissolved molecular CO_2 is also present in these Ne glasses (representing <1 wt% of total dissolved CO_2). Figure 2b compares clear and blackened glasses prepared at similar conditions. The blackened samples have reduced amounts of molecular CO_2 and display a new IR peak (at ~ 2185 cm^{-1} or 2135 cm^{-1} for ^{12}C and ^{13}C samples, respectively), which can be assigned to dissolved CO (Nakamoto 1978; Brooker et al., unpublished data). At any given set of conditions, less intense CO peaks also may be found in clear samples, indicating minor reduction prior to graphite saturation.

If the fluid composition in these experiments has evolved due to infiltration of H_2 , the approximate amount of H_2O expected in the capsule before graphite precipitates can be estimated by calculating the molar proportions of volatile species. The theoretical fluid composition along the CO_2 - H_2 join at 2.5 GPa and 1650 $^\circ\text{C}$, and the intersection with the graphite stability field are shown in Figures 3a and 3b. Hydrogen infiltration into a pure CO_2 fluid would initially result in the formation of equimolar quantities of CO and H_2O as in the following reaction:



At graphite saturation, the relative quantities of H_2 required and H_2O produced in the example in Figure 3b are approximately as follows (ignoring minor H_2 and CH_4 in the product):



The 2.5 GPa Ne sample had a bulk-loaded weight of 0.2 g, including 0.027 g of CO_2 (13.5 wt%). At 2.5 GPa, assuming that all the loaded CO_2 is involved (and disregarding slight differences in volatile activity in melt and fluid phase), 0.49 mg of H_2 are required to reach graphite saturation, resulting in the formation of 4.4 mg of H_2O . An insignificant fraction of this H_2O will partition into

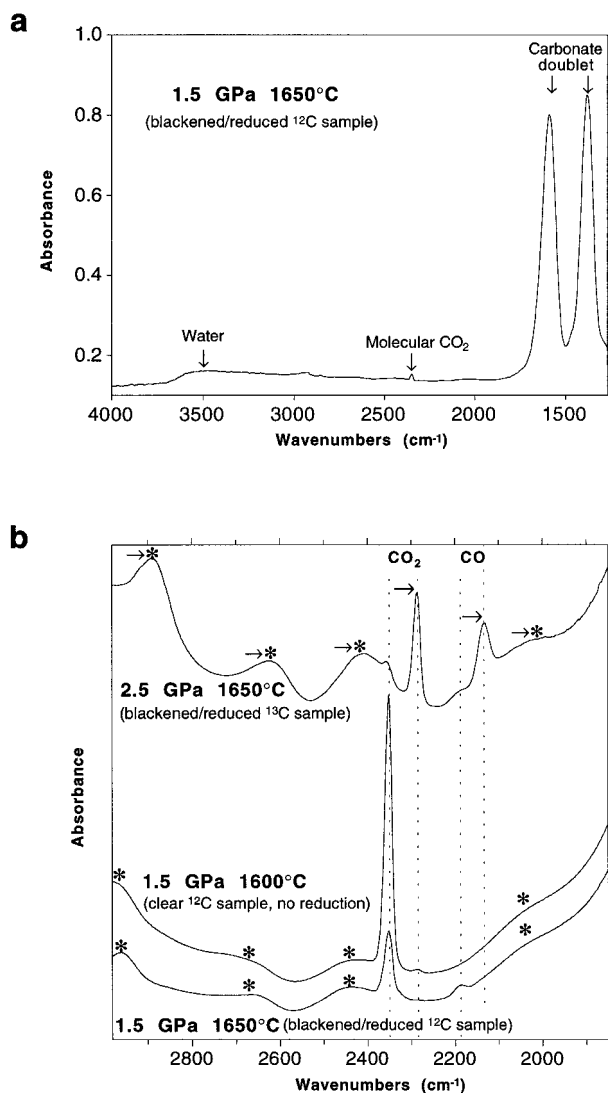


FIGURE 2. IR spectra of Ne ($\text{NaAlSiO}_4 + {}^{12}\text{CO}_2$) glasses. (a) Neon sample prepared at 1.5 GPa and 1650 °C. The intensity of the broad peak at 3500 cm^{-1} indicates an H_2O content of 0.15 wt% (calculated using the extinction coefficient of 70 $\text{L}\cdot\text{mol}^{-1}\cdot\text{cm}^{-1}$ from Silver and Stolper 1989). The carbonate doublet peaks at 1600 and 1375 cm^{-1} represent 1.90 wt% dissolved CO_2 (using an extinction coefficient of 282 $\text{L}\cdot\text{mol}^{-1}\cdot\text{cm}^{-1}$ for the 1600 cm^{-1} peak from Brooker et al., unpublished data). The minor feature at 2351 cm^{-1} represents a small amount of dissolved molecular CO_2 . (b) The minor molecular CO_2 peaks are shown in detail along with peaks assigned to dissolved ${}^{12}\text{CO}$ at 2185 cm^{-1} and ${}^{13}\text{CO}$ at 2135 cm^{-1} . The bottom two spectra illustrate the dramatic decrease in molecular CO_2 with graphite saturation and the simultaneous appearance of a small CO peak. The top spectrum illustrates the large increase in $\text{CO}:\text{CO}_2$ intensity ratio as expected for the higher f_{CO} at 2.5 GPa (even though the $\text{CO}:\text{CO}_2$ ratio of the graphite-saturated fluid is actually reduced; see Fig. 3b). The peaks marked with an asterisk are carbonate overtones and the arrows indicate the isotopic shift for all C related peaks.

the excess fluid phase and the majority will dissolve in the melt to give an H_2O concentration approaching 2.5 wt% (below saturation at these conditions; e.g., McMillan and Holloway 1987). Given the significantly lower H_2O content observed in the sample (0.1 wt%), infiltration of H_2 cannot be responsible for graphite precipitation. The H_2O content is also constant across the sample, in contrast to the diffusion gradient expected if H_2 was continuing to enter the capsule from outside, prior to equilibration (cf. Stolper et al. 1987).

Figure 3b illustrates that graphite would not be precipitated by infiltration of H_2 for the blackened Ne sample prepared at 1.5 GPa and 1650 °C, because the graphite saturation curve fails to intersect the $\text{CO}_2\text{-H}_2$ join for these conditions. The range of $P\text{-}T$ conditions for which the graphite saturation curve and the $\text{CO}_2\text{-H}_2$ join do not intersect is estimated in Figure 3c. Of the “failed” blackened glasses prepared during the study of Brooker et al. (unpublished data), the observed H_2O contents of all samples (0.1–0.3 wt%) are insufficient to justify the production of graphite by the reactions in Equations 1 and 2, even when the $P\text{-}T$ conditions are appropriate (see Fig. 3c). Although a minor amount of H_2 infiltration may still occur in these experiments, it appears to be negligible for carefully dried, anhydrous piston-cylinder assemblies and will not contribute significantly to any reduction or graphite precipitation. The homogeneously distributed H_2O content observed for the samples of Brooker et al. (unpublished data) probably represents H_2O adsorbed onto the surface of the starting material. Water contents of ~0.1–0.3 wt% appear lower than in many other studies (e.g., Stolper et al. 1987; Taylor 1990), possibly due to the use of a carbonate starting material, which compared to the silver oxalate used in some other studies is easy to obtain and store in an anhydrous form. The dry mixing and loading of starting materials within an oven also may be important. Obviously, high H_2O totals in other studies could represent infiltration of H_2 related to differences in experimental design or procedures. In general, the loaded H_2O contents must be estimated and subtracted before any infiltration of H_2 can be assessed.

The observations presented above appear to exclude the process of H_2 infiltration as a cause of reduction in these experiments and some other reducing agent must be responsible; the most obvious candidate is infiltration by C as shown by the reaction in Equation 3. Some of the initial experiments of Brooker et al. (unpublished data) and Kohn et al. (1991), which utilized 99% ${}^{13}\text{C}$ -enriched Na_2CO_3 , did produce clear graphite-free glasses but unexpectedly large IR absorbance peaks for ${}^{12}\text{C}$ species were noted in these samples. The spatial distribution of ${}^{12}\text{C}$ enrichment suggested a substantial influx of ${}^{12}\text{C}$ through the capsule wall from an external source, possibly the graphite furnace. This would be consistent with the observations of Watson et al. (1982) and Watson (1987) who demonstrated the mobility of C through Pt, although both these studies suggested C loss rather than infiltration for piston-cylinder experiments.

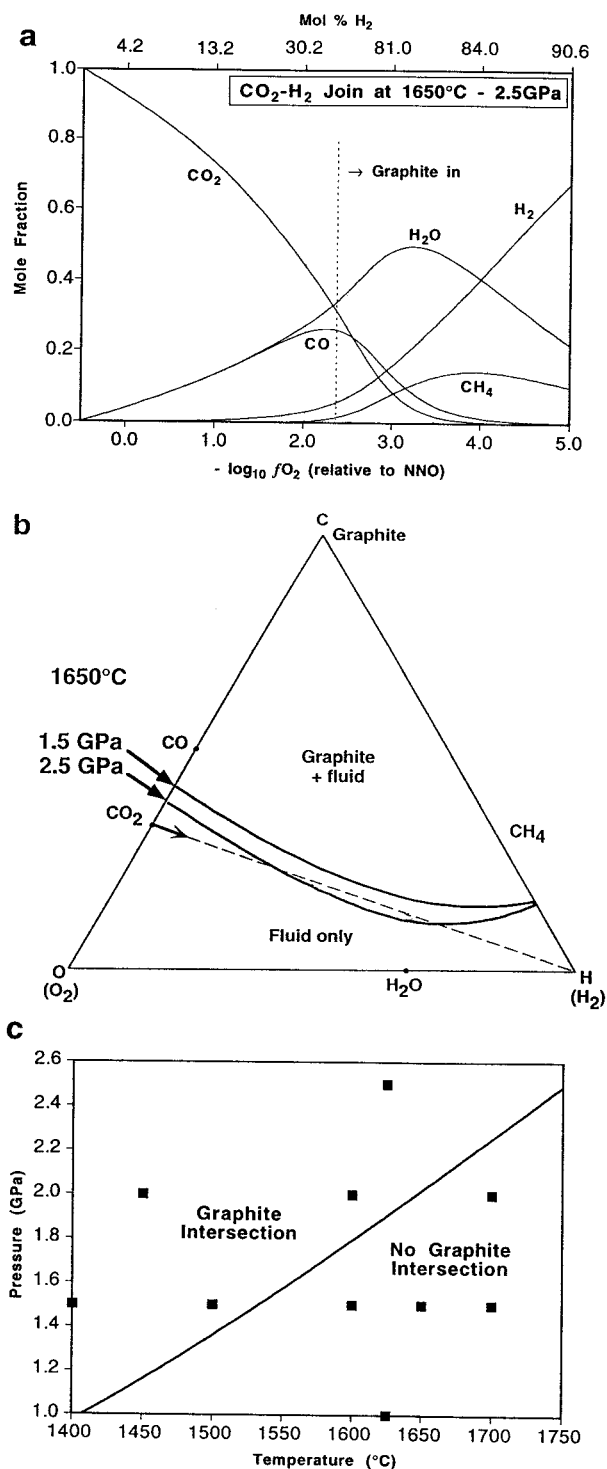


FIGURE 3. Theoretical changes in the composition of an initially pure CO₂ fluid as H₂ is added to the system. **(a)** The fluid composition along the CO₂-H₂ join at 2.5 GPa and 1650 °C. Note that the initial addition of H₂ produces equal proportions of CO and H₂O. **(b)** The C-O-H ternary diagram at 1650 °C illustrating the intersection of the CO₂-H₂ join with the graphite saturation curve at 2.5 GPa but not at 1.5 GPa. **(c)** The *P-T* conditions for which the graphite stability region intersects the CO₂-H₂ join as approached from the CO₂ direction. Squares indicate the conditions of blackened experiments produced during the study of Brooker et al. (unpublished data). Calculations follow the method of Holloway (1987); the positions of all curves are dependent on the equations of state used, which for these examples are from Saxena and Fei (1987).

←

a function of C activity and oxidation gradient across the platinum wall. For these experiments, a Jd composition was selected because this composition commonly displayed blackened rims progressing into the glass from the capsule wall in experiments of about 30 min durations. This feature would allow the identification of differences between blackened and clear areas of the sample.

In the first experiment, a platinum capsule containing a Jd + ¹³CO₂ mixture was sealed inside an outer capsule containing a powdered graphite furnace of natural isotopic abundance, (98.9% ¹²C). After being held at 2.0 GPa and 1600 °C for 20 min, the quenched glass had a thin blackened rim (50–100 μm) evenly distributed around the charge resulting from a distribution of black particles (identified as graphite by Raman spectroscopy) just visible at 500× magnification. The IR and SIMS profiles, which are shown in Figures 4 and 5, demonstrate the progressive infiltration of ¹²C for a horizontal section through the middle of the inner capsule. The intensity of the IR absorbance at 3500 cm⁻¹ (Fig. 4c) is constant across the capsule suggesting that the H₂O content (0.15–0.12 wt%) is a loaded component (although equilibrium could have been reached between the inner capsule and an external source of H₂O). Small peaks visible at ~2150 and ~2100 cm⁻¹ can be assigned to dissolved molecular ¹²CO and ¹³CO, respectively, even though they are in slightly different positions relative to the CO peaks in the Ne composition (see Fig. 2b). Detailed examination indicates that these CO peaks display the same isotopic spatial distribution as seen for the molecular CO₂ and carbonate species. It should be noted that only a ¹³CO peak is present in the center of the sample suggesting that this area was in chemical, but not isotopic equilibrium with the graphite (¹²C) at the edge of the charge.

¹²C SIMS imaging of the inner platinum capsule wall indicated relatively high concentrations of C along grain boundaries, which probably represent the main transport path through the Pt as suggested by Watson (1987). With such a complex pathway, it is not possible to estimate boundary conditions and determine diffusion coefficients accurately from the available data. The isotopic diffusion profile evident in Figure 5 progresses further into the

Isotopic tracers

Two double capsule, isotopic tracer experiments were designed to: (1) confirm the process of C migration into an experiment to produce reduction; (2) demonstrate the extent of infiltration on the time scale of these experiments; and (3) determine the mobility of C through Pt as

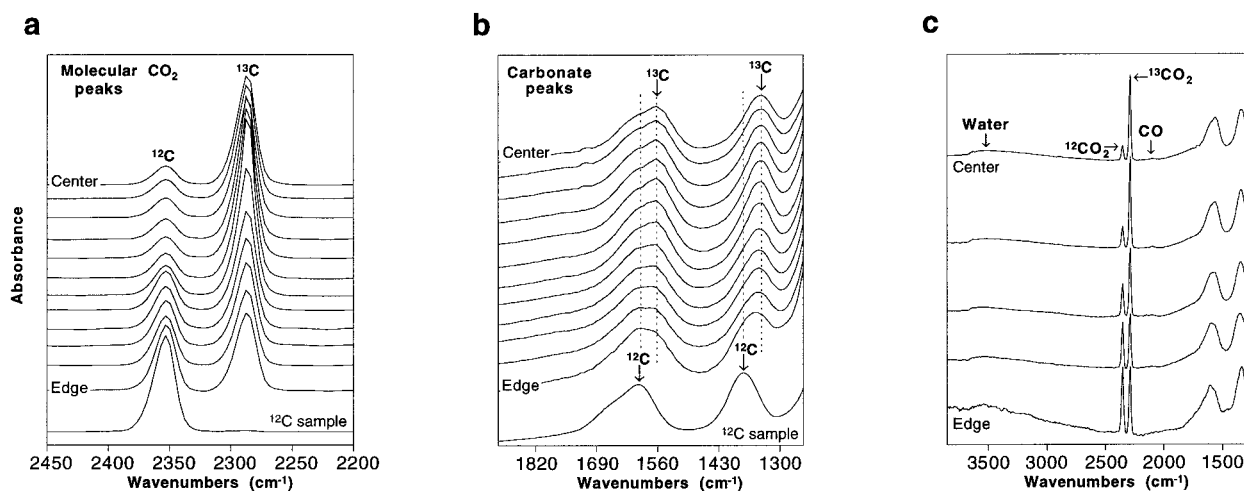


FIGURE 4. IR spectra showing the isotopic tracer diffusion of “external” ¹²C entering a ¹³C Jd melt through the platinum capsule wall. The spectra represent consecutive 55 μm squares along a horizontal section through the middle of the Jd + ¹³CO₂ composition glass. **(a)** The peaks at 2352 and 2283 cm⁻¹ represent dissolved molecular ¹²CO₂ and ¹³CO₂ species, respectively. **(b)** The broader peaks at ~1600 and 1350 cm⁻¹ represent carbonate, the positions of individual isotopic components are indicated but difficult to resolve. **(c)** Selected spectra are shown for a wider wavenumber range to illustrate the low and constant H₂O content as indicated by the intensity of the band at 3500 cm⁻¹. The small peaks just visible at 2150 and 2100 cm⁻¹ are assigned to dissolved molecular ¹²CO and ¹³CO (Brooker et al., unpublished data). The spectrum from the very edge of the sample is for a smaller cross sectional area and is consequently of poor quality. The total CO₂ dissolved is difficult to determine in this sample as the molar absorptivities for ¹³C species are not known, but an approximate estimate of ~1.3–1.4 wt% can be made using the ¹²C molar absorptivities of Fine and Stolper (1985) and this appears approximately constant across the profile. Natural abundance ¹²C spectra are shown for comparison in **(a)** and **(b)**.

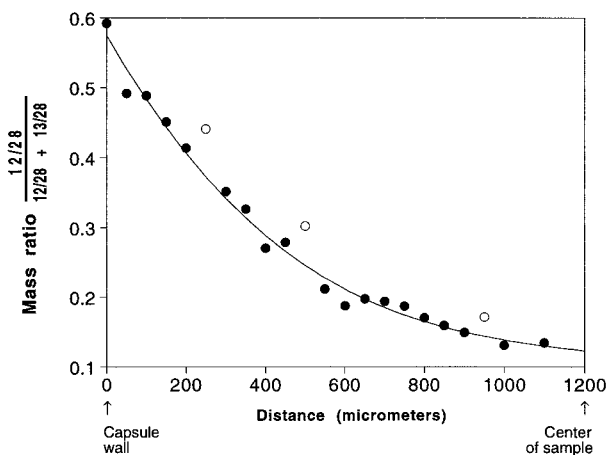


FIGURE 5. The SIMS data showing ¹²C infiltration along the same profile represented in Figure 4. Masses 12 and 13 are normalized to mass 28 (Si) in the Jd glass. It should be noted that it was possible to avoid particles of disseminated C at the edge of the sample. Open circles are data points omitted from the curve fit as these appear to represent anomalies possibly related to ¹²C surface contamination (associated with high H count rates). A similar shaped profile can be derived from the ratio of the molecular CO₂ peaks in Figure 4, although uncertainty in the molar absorptivity for ¹³CO₂ and the lower spatial resolution provide a less quantitative result.

charge than the visible blackening, but clearly lacks the sigmoidal shape expected for a simple diffusion process. Taking the raw data as seen, the fitted line in Figure 5 can be modeled by a rapid penetration of ¹²C deep into the sample, possibly isotopic tracer diffusion at $\sim 1.7 \times 10^{-5}$ cm²/s, which is overprinted by a slower secondary process at a rate of $\sim 2.7 \times 10^{-7}$ cm²/s, more consistent with the chemical diffusion rates for carbonate and molecular CO₂ species (see Watson 1994). However, time dependent changes in the permeability of the Pt (annealing) may also be responsible for the complexity of the diffusion profile.

Approximate estimates of the flux rate of C through the platinum capsule (using the diffusion/permeability data of Watson 1987) confirm that enough C can enter the capsule during the experiment to satisfy easily the mass balance requirements of Equation 3. However, considering diffusion in terms of chemical potential gradients, it is interesting to note that the activity of C inside the capsule approaches a value of 1 as the first molecule of graphite becomes stable (Eq. 3), and no thermodynamic driving force should exist across the capsule wall from the external powdered graphite (also activity = 1). As a result, diffusion might be expected to stop as soon as the first particle of graphite is formed in the capsule. The variable entropy associated with the change in graphite defect type or particle size is one possible factor that may affect the thermodynamic equilibrium (note that any thermal gradient across the capsule wall would not affect the

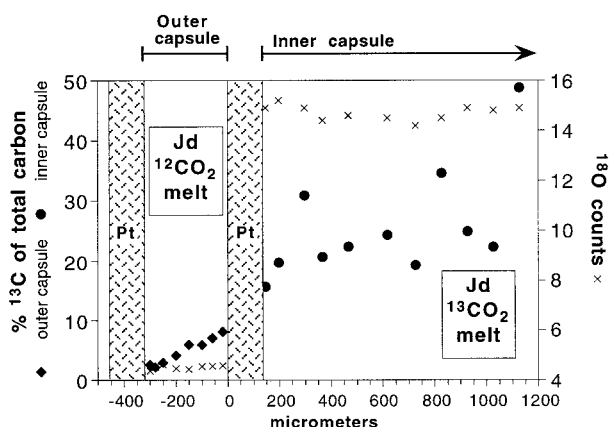


FIGURE 6. The isotopic tracer diffusion of ^{13}C from an “external” Jd + $^{12}\text{CO}_2$ melt, migrating through a platinum capsule wall to enter a Jd + $^{13}\text{CO}_2$ melt as demonstrated by the SIMS profile along a horizontal section through both inner and outer capsules. The counts recorded for ^{18}O (arbitrary units) at each data point are indicated by crosses.

activity). It is clear from this experiment that there is a mass transfer of C through the Pt that continues after the reaction in Equation 3 has been completed and graphite is a stable phase in the inner capsule.

It is interesting to note that the platinum capsules of Watson et al. (1982) were surrounded by graphite. Although the transfer of ^{14}C out of the capsule was reported, there was no mention of blackening of the glass charge related to the concomitant influx of ^{12}C , which should have occurred (as suggested by Watson 1987, p. 490).

In a double-capsule experiment similar to the one above, CO_2 -bearing glasses were placed on either side of a platinum wall to determine if C migration occurs without a difference in oxidation state to act as the driving force. A Jd + $^{13}\text{CO}_2$ starting composition was placed in the inner capsule and surrounded by a Jd + $^{12}\text{CO}_2$ mix in the outer capsule. This arrangement was held at 2.0 GPa and 1600 °C for 30 min. Figure 6 illustrates an ion probe profile across the resultant glasses, in which the outer $^{12}\text{CO}_2$ glass shows a progressive increase in ^{13}C contamination that approaches ~10% adjacent to the inner capsule. The inner $^{13}\text{CO}_2$ glass shows a range of ^{13}C contamination from about 10% to above 30%, although the profile is not as linear as the sample in Figure 5 (possibly due to convection or the complex shape of the capsule). Graphite and CO were not detected in either of the glasses (note there is no detectable ^{13}C infiltration from the furnace in this particular experiment). These results demonstrate that isotopic exchange between oxidized C species can occur through Pt. Although elemental C is presumably present within the capsule wall, it is not in chemical equilibrium with the melts on either side (i.e., no CO is produced as required by Eq. 3). It is unlikely that large CO_2 molecules could diffuse through Pt and this is confirmed by the containment of the ^{18}O -enrichment (a characteristic of the ^{13}C -enriched carbonate start-

ing material) in the inner capsule (Fig. 6). It is reassuring to note that O will not transfer through Pt as this would have profound implications for many experimental studies.

DISCUSSION

IR and NMR peaks related to CO have been identified for all blackened NaAlO_2 - SiO_2 compositions prepared during the study of Brooker et al. (unpublished data). This has proved a valuable indicator of the progress of reactions in Equations 1, 2, and 3. The presence of relatively minor amounts of CO in a sample can be used to identify the onset of reduction in clear samples that have not reached graphite saturation (i.e., the reaction in Eq. 2 or 3 has not been completed). With the identification of C as the reducing agent in the blackened experiments and the ability to analyze samples for signs of even minor reduction, it also has been possible to evaluate the causes of intermittent infiltration of C in the Brooker et al. (unpublished data) experiments. This has allowed us to monitor the success of various modifications to assembly design, and a variety of factors appear to be important.

Factors that contribute to C infiltration

One important factor to be considered is the intermittent nature of C infiltration. The electrical power requirements of the graphite furnace appear to indicate a significant problem, as relatively high voltages (and low currents) are commonly associated with blackened samples. The voltage may have been relatively high throughout the heating cycle, or show a sudden increase after a stable period. However, the voltage is generally observed to increase suddenly as the temperature approaches 1550 °C. This voltage increase may be preceded by an apparent increase in the measured pressure. Experiments often fail as the voltage suddenly increases but in some cases they last for tens of minutes even at 1625 °C.

Due to deformation during isobaric quenching and extraction from the pressure vessel, it is difficult to identify any specific furnace damage related to failed experiments or blackened samples. However, the Pyrex that is around and above the capsule (see Fig. 1) sometimes showed blackened rims or swirling streaks (similar to Jd samples) that appeared to emanate from point locations on the furnace wall. In some cases the Pyrex also appeared to have flowed into fractures in the furnace that must have been present during the experiment. These furnace defects may play an important role in controlling the release of mobile C, and the decreased viscosity of Pyrex at high temperatures may also assist the migration of C particles toward the capsule. Migration of C also has been noted for other assembly designs and, at high temperatures, a graphite furnace has been seen to disseminate into the NaCl if the intervening Pyrex sleeve is not present.

In contrast to the situation above, where C appears to migrate through the Pyrex to the capsule, blackened samples inevitably resulted from an obvious contact between the capsule and the furnace during high-temperature ex-

periments. This situation was also associated with a high power requirement for the furnace. The Pt was commonly "shiny" at the point of contact for experiments between 1550–1650 °C, with melting and breaching of the capsule at higher temperatures. It is not clear whether the melting point of Pt is reduced by dissolved C (see below) or the contact causes a furnace hot spot.

In general, it appears that the proximity of the capsule and the condition of the furnace will determine whether C accesses a capsule on a short time scale (10–30 min). However, it also has been noted that in some experiments there are more subtle deterioration features (changes in power requirements) that operate on a longer time scale (several hours) and eventually lead to mobility of C, reduction of samples, and possibly the ultimate failure of the experiment.

Limiting infiltration and reduction

The above observations demonstrate the importance of the capsule-furnace environment, and the following procedures and assembly modifications appear to restrict mobility of C and access to the capsule. In general, two main factors must be controlled in this type of experiment: the deformation characteristics of the assembly during the pressurization/heating cycle, and the degree of physical isolation experienced by the capsule.

Application of pressure and temperature. It would appear that the condition of the furnace throughout an experiment is a critical factor in limiting the mobility of C. The initial application of pressure and temperature can have a major effect on the condition of the furnace. For the particular assembly used in Figure 1, as well as the modified version described below, the following procedure was found to be particularly successful: cold pressurization to about 0.7 GPa, then heating to 550 °C (Pyrex soft but not mobile) followed by careful and slow application of the final pressure (or excess pressure) and heating to the desired temperature, ensuring no pressure is lost at any point. Any major loss in pressure appears to damage the furnace and at lower pressures (≤ 1.0 GPa), capsules with excess volatiles may also explode. Any attempt to overpressurize and bleed off the excess pressure at the final temperature ("hot piston out") must be done with extreme caution. It should be noted that different procedures may be more suited to different assembly designs or to different experimental conditions

Mechanical strength around the capsule. With the arrangement in Figure 1, the most critical aspect of assembly construction is to ensure that the capsule is not touching the furnace. In addition, the assembly must also fit together well (no collapsible space) and the capsule should deform evenly during pressurization, which is best ensured by carefully "pre-squashing" the capsule in a small press before loading.

In some cases, powdered materials other than Pyrex have been used around capsules. In this laboratory, alumina powder or mixtures of alumina and MnO_2 powder have been investigated, and Rosenbaum and Slagel

(1995) have used mixtures of NaCl or BaCO_3 powder with hematite or tantalum. Because some of these techniques have merit as hydrogen "getters" in place of a double capsule, they may eliminate one source of reduction in some experiments (e.g., with hydrous assembly materials). However, attempts to use various powders in this laboratory at high temperatures have produced intermittent results, some powders appeared to reduce the occurrence of blackening, but not to eliminate the problem completely. Again, the power requirement of the furnace indicates damage for the experiments with blackened samples, but the anomalous power consumption is often apparent as soon as the current is switched on. This possibly reflects a low mechanical strength and inward collapse of the furnace during pressurization as opposed to a mechanical instability occurring for the Pyrex as it becomes mobile during heating. Reduction was noted in the Geophysical Lab assembly when the boron nitride sleeve was replaced with other materials (Eggler et al. 1974). This may have resulted from a reduction in mechanical strength around the furnace rather than the removal of a H_2 sink, as claimed by Eggler et al. (1974).

Because the most severe cases of C infiltration involve the obvious contact of the capsule with the furnace or migration of solid carbon particles through the Pyrex, the assembly in Figure 1 was modified to the configuration originally used in this and many other laboratories, with a crushable alumina sleeve replacing the Pyrex around the capsule. However, a 4.6 mm diameter capsule is used instead of 5 mm, leaving room for a substantial, 0.8 mm thick, crushable alumina sleeve between the capsule and the furnace (less substantial alumina sleeves were not as effective). This represents a slight compromise because the sample volume is reduced by about 20% (but less than the reduction for the double capsule technique). This design modification appears to maintain the furnace in good condition as well as avoiding contact with the capsule. Successful experiment durations of 2 h at 1600 °C and 30 min at 1750 °C are easily attained (in our laboratory experiment durations are limited by the high external temperature eventually reached by the apparatus). Using these precautions, over 90% of glasses prepared in the $\text{NaAlO}_2\text{-SiO}_2$ system have been free of blackening and CO-related IR peaks are insignificant.

The advantages of isolating a capsule with alumina also have been noted by Presnall et al. (1973). They showed that encased platinum capsules can be used at 1800 °C for 2 h (even 1825 °C for several minutes) in piston-cylinder experiments, instead of the 1600–1625 °C maximum often quoted by others (e.g., Williams and Kennedy 1969). Presnall et al. (1973) suggest that this is due to isolation from some undefined contaminant. Platinum metal can dissolve as much as 1.2 wt% C at 1 bar (see Massalski 1986, p 581), which depresses the melting point from 1770 to 1705 °C. The effect may be exaggerated at higher pressures and C may be the contaminant noted by Presnall et al. (1973). It should also be noted

that any Fe present in the Pt may produce an even lower ternary eutectic melting temperature.

Replacing the Pyrex with an alumina sleeve eliminates another problem noted in this and other laboratories (e.g., Silver and Stolper 1989), which is boron contamination from the Pyrex (12 wt% as B₂O₃ in Pyrex). Diffusion of this element through the platinum has been identified by SIMS analysis and concentrations as high as 1–2 wt% have been measured in glasses adjacent to the capsule wall (Hervig, unpublished data). The use of a crushable alumina sleeve around the capsule and a 1 mm thick crushable alumina disk above appears to isolate the capsule from any boron contamination related to Pyrex in the assembly.

Although the use of alumina appears satisfactory for the type of experiment described in this study, Watson (1986) has noted a relatively high solubility and mobility for C in polycrystalline alumina compared to polycrystalline olivine, and a sleeve of dunite may prove even more effective as a barrier to C.

As well as increasing the risk of furnace damage, high temperatures may play an important role in controlling the mobility of furnace C through materials surrounding a capsule as well as the diffusion rate through the platinum capsule wall. It is not yet clear if there is a temperature (<1450 °C) that represents a minimum prerequisite for infiltration of C. Rosenbaum and Slagel (1995) did not identify infiltration of C in single capsule experiments at 1000 °C, but it is possible that a badly damaged furnace might result in infiltration of C either at lower temperatures (<1450 °C) or on a longer time scale.

The results of this study (and results of Rosenbaum and Slagel 1995) suggest that for nominally anhydrous assemblies, the supply of H₂ is limited and infiltration of this component is minimal, possibly below the level allowed by “buffered” double capsules. The success of double capsules containing “*f*_{o₂} buffers” may reflect their presence as a physical barrier to solid C rather than a chemical buffer for H₂. As a result, double capsules appear unnecessary for most applications where dry NaCl/Pyrex assemblies can be used and C mobility is controlled.

Capsule and furnace materials. Other capsule materials that might limit C (and H₂) entry can be used in some circumstances. The diffusion rate of C through Au or Ag at high temperatures and pressures is unknown but, by analogy with H₂, it may be significantly lower than the diffusion rate through Pt (and Pd). However, the low melting point of these materials limits their use for the high-temperature experiments where C infiltration appears to be a potential problem.

Carbon infiltration has not yet been identified for Fe-bearing compositions prepared in this laboratory, even for capsules surrounded by Pyrex as in Figure 1. This may be related to the Fe²⁺/Fe³⁺ ratio of the starting material, which is commonly high enough to buffer the sample and oxidize any incoming C (or H₂) for some finite time. For CO₂ solubility experiments on Fe-bearing compositions,

the oxidized C will accumulate with the loaded (excess) CO₂ until the Fe²⁺/Fe³⁺ ratio of the melt requires CO to be stable. For nominally volatile-free Fe-bearing melts, the oxidized C may produce unexpected CO₂ (c.f. Holloway et al. 1992), which may not be identified unless samples are examined by IR spectroscopy. However, it also should be noted that platinum capsules used for Fe-bearing experiments are generally pre-doped with Fe or become Fe-saturated during the experiment and it is also possible that the Fe-doped Pt is less permeable to C.

One way to eliminate the source of C contamination is to replace the graphite furnace. Preliminary testing of an Inconel 600 nimonic alloy furnace has been promising and a thin foil (0.075 mm) furnace has very similar resistive properties to graphite, requiring no adjustment of the apparatus power supply. However, the maximum temperature possible at 2.0 GPa appears to be about 1450 °C. Attempts to use lanthanum chromite have proved unsuccessful due to the very different and non-linear (with temperature) resistive properties of this material. As a result, a very thin furnace may be required and it is doubtful that this would survive pressurization. Rhenium foil is another possible furnace material (used in this laboratory for multi-anvil assemblies), although the strong temperature dependence of resistivity (giving large thermal gradients) and the large expense for a piston-cylinder-sized furnace prohibit interest in this option.

ACKNOWLEDGMENTS

We would like to thank Paul McMillan (ASU) and Mike Carroll (Bristol) for access to Raman and FTIR spectrometers. Helpful comments were made by Todd Dunn, Simon Kohn, and Bruce Watson. This study was initiated at ASU where R.A.B. was supported by NASA grant MPA0092 and completed at Bristol where R.A.B. was supported by NERC grant GR3/09695.

REFERENCES CITED

- Allen, J.C., Modreski, P.J., Haygood, C., and Boettcher, A.L. (1972) The role of water in the mantle of the earth: the stability of amphiboles and micas. International Geological Congress Report, 24th session, 2, 231–240.
- Boettcher, A.L. (1984) The system SiO₂-H₂O-CO₂: melting, solubility mechanisms of carbon, and liquid structure to high pressure. *American Mineralogist*, 69, 823–833.
- Brey, G. (1976) CO₂ solubility and solubility mechanisms in silicate melts at high pressures. *Contributions to Mineralogy and Petrology*, 57, 215–221.
- Brey, G. and Green, D.H. (1976) Solubility of CO₂ in olivine melilitite at high pressures and the role of CO in the Earth's upper mantle. *Contributions to Mineralogy and Petrology*, 55, 217–230.
- Eggler, D.H., Mysen, B.O., and Hoering, T.C. (1974) Gas species in sealed capsules in solid media, high pressure apparatus. *Carnegie Institution of Washington Yearbook*, 73, 228–232.
- Eugster, H.P. (1957) Heterogeneous reactions involving oxidation and reduction at high pressures and temperatures. *Journal of Chemical Physics*, 26, 1760–1761.
- Fine, G. and Stolper, E. (1985) The speciation of carbon dioxide in sodium aluminosilicate glasses. *Contributions to Mineralogy and Petrology*, 91, 105–121.
- Holloway, J.R. (1987) Igneous fluids. In *Mineralogical Society of America Reviews in Mineralogy*, 17, 182–186.
- Holloway, J.R., Mysen, B.O., and Eggler, D.H. (1976) The solubility of

- CO₂ in liquids on the join CaO-MgO-SiO₂-CO₂. *Carnegie Institution of Washington Yearbook*, 75, 626–631.
- Holloway, J.R., Pan, V., and Gudmundsson, G. (1992) High-pressure fluid-absent melting experiments in the presence of graphite: oxygen fugacity, ferric/ferrous ratio and dissolved CO₂. *European Journal of Mineralogy*, 4, 105–114.
- Kohn, S.C., Brooker, R.A., and Dupree, R. (1991) ¹³C MAS NMR: A method for studying CO₂ speciation in glasses. *Geochimica et Cosmochimica Acta*, 55, 3879–3884.
- Luth, R.W. (1989) Natural versus experimental control of oxidation state: Effects on the composition and speciation of C-O-H fluids. *American Mineralogist*, 74, 50–57.
- McMillan, P.F. and Holloway, J.R. (1987) Water solubility in aluminosilicate melts. *Contributions to Mineralogy and Petrology*, 97, 320–332.
- Massalski, T.B. (1986) *Binary Alloy Phase Diagrams*. American Society for Metals, vol. 1, Ohio, U.S.A.
- Mattey, D.P. (1991) Carbon dioxide solubility and carbon isotope fractionation in basaltic melt. *Geochimica et Cosmochimica Acta*, 55, 3467–3473.
- Mattey, D.P., Taylor, W.R., Green, D.H., and Pillinger, C.T. (1990) Carbon isotopic fractionation between CO₂, vapour, silicate and carbonate melts: an experimental study to 31 kbar. *Contributions to Mineralogy and Petrology*, 104, 492–505.
- Merrill, R.B. and Wyllie, P.J. (1974) Kaersutite and kaersutite eclogite from Kakanui, New Zealand; water-excess and water deficient melting to 30 kilobars. *Geological Society of America Bulletin*, 86, 555–570.
- Mysen, B.O. (1976) The role of volatiles in silicate melts: solubility of carbon dioxide and water in feldspar, pyroxene and feldspathoid melts to 30 kb and 1625°C. *American Journal of Science*, 276, 969–996.
- Mysen, B.O., Eggler, D.H., Seitz, M.G., and Holloway, J.R. (1976) Carbon dioxide in silicate melts and crystals. Part 1: Solubility measurements. *American Journal of Science*, 276, 455–479.
- Nakamoto, K. (1978) *Infrared and Raman spectra of inorganic and coordination compounds*. (3rd Ed.), 448 p. Wiley, New York.
- Presnall, D.C., Brenner, N.L., and O'Donnell, T.H. (1973) Drift of Pt/Pt10Rh and W3Re/W25Re thermocouples in single stage piston-cylinder apparatus. *American Mineralogist*, 58, 771–777.
- Rosenbaum, J.M. and Slagel, M.M. (1995) C-O-H speciation in piston-cylinder experiments. *American Mineralogist*, 80, 109–114.
- Saxena, S.K. and Fei, Y. (1987) High pressure and high temperature fluid fugacities. *Geochimica et Cosmochimica Acta*, 51, 783–791.
- Silver, L.A. and Stolper, E.M. (1989) Water in albitic glasses. *Journal of Petrology*, 30, 667–709.
- Sneeringer, M.A. and Watson, E.B. (1985) Milk cartons and ash cans: two unconventional welding techniques. *American Mineralogist*, 70, 200–201.
- Stolper, E., Fine, G., Johnson, T., and Newman, S. (1987) Solubility of carbon dioxide in albitic melt. *American Mineralogist*, 72, 1071–1085.
- Taylor, W.R. (1990) The dissolution mechanism of CO₂ in aluminosilicate melts-infrared spectroscopic constraints on the cationic environment of dissolved (CO₃)²⁻. *European Journal of Mineralogy*, 2, 547–563.
- Watson, E.B. (1986) Immobility of reduced carbon along grain boundaries in dunite. *Geophysical Research Letters*, 13, 529–532.
- (1987) Diffusion and solubility of C in Pt. *American Mineralogist*, 72, 487–490.
- (1994) Diffusion in volatile-bearing magmas. In *Mineralogical Society of America Reviews in Mineralogy*, 30, 371–411.
- Watson, E.B., Sneeringer, M.A., and Ross, A. (1982) Diffusion of dissolved carbonate in magmas: experimental results and applications. *Earth and Planetary Science Letters*, 61, 346–358.
- Wendlandt, R.F., Huebner, J.S., and Harrison, W.J. (1982) The redox potential of boron nitride and implications for its use as a crucible material in experimental petrology. *American Mineralogist*, 67, 170–174.
- Williams, D.W. and Kennedy, G.C. (1969) Melting curve of diopside to 50 kilobars. *Journal of Geophysical Research*, 74, 4359–4366.

MANUSCRIPT RECEIVED SEPTEMBER 23, 1997

MANUSCRIPT ACCEPTED MAY 8, 1998

PAPER HANDLED BY ROBERT W. LUTH